ESTIMATION OF ABOVEGROUND CARBON STOCK USING SAR SENTINEL-1 IMAGERY IN SAMARINDA CITY

Bayu Elwantyo Bagus Dewantoro[1]*, Retnadi Heru Jatmiko[1]
[1]Department of Geographic Information Science, Faculty of Geography, Universitas Gadjah Mada, Yogyakarta, 55281, Indonesia
*e-mail: bayuelwantyo@mail.ugm.ac.id
Received: 2 May 2021; Revised: 8 July 2021; Approved: 13 August 2021

Abstract. Estimation of aboveground carbon stock on stands vegetation, especially in green open space, has become an urgent issue in the effort to calculate, monitor, manage, and evaluate carbon stocks, especially in a massive urban area such as Samarinda City, Kalimantan Timur Province, Indonesia. The use of Sentinel-1 imagery was maximised to accommodate the weaknesses in its optical imagery, and combined with its ability to produce cloud-free imagery and minimal atmospheric influence. The study aims to test the accuracy of the estimated model of above-ground carbon stocks, to ascertain the total carbon stock, and to map the spatial distribution of carbon stocks on stands vegetation in Samarinda City. The methods used included empirical modelling of carbon stocks and statistical analysis comparing backscatter values and actual carbon stocks in the field using VV and VH polarisation. Model accuracy tests were performed using the standard error of estimate in independent accuracy test samples. The results show that Samarinda Utara subdistrict had the highest carbon stock of 3,765,255.9 tons in the VH exponential model. Total carbon stocks in the exponential VH models were 6,489,478.1 tons, with the highest maximum accuracy of 87.6 %, and an estimated error of 0.57 tons/pixel.

Keywords: *carbon stock estimation, statistical analysis, remote sensing, Sentinel-1 imagery, Samarinda City.*

1 INTRODUCTION

Stands vegetation in a city contributes greatly to the suppression of adverse impacts of urban activity, and to improved environmental quality and health in urban areas, including improved air quality, energy conservation, lower air temperatures, and ultraviolet radiation (Tavasoli, N., Arefi, H., Samiei-Esfahany, S., & Ronoud, Q., 2019). Stands vegetation in green open space also acts as a natural carbon sink in urban areas, which is very beneficial for climate change mitigation because of its ability to absorb carbon dioxide (CO_2) from the atmosphere (Godwin et al., 2015; Poudyal et al., 2011; Strohbach & Haase, 2012). This makes the provision, monitoring, and evaluation of biomass content and carbon stocks capable of playing a role in the absorption of inorganic carbon in urban areas in stands vegetation a serious concern (Jo, 2002, in Wang & Gao, 2020).

The measurement of aboveground biomass (AGB) and carbon stocks has been made by many researchers with a variety of methods, such as direct measurements in the field of the characteristics of biological vegetation structures (Fonseca et al., 2012 in Van Pham et al., 2019) or destructive measurements of vegetation samples capable of extracting important features in the calculation of AGB (Chave et al., 2014). Quantitative approaches have included canopy models and vegetation types (Krooks et al., 2014) and allometric equations using remote sensing techniques integrated with data

http://dx.doi.org/10.30536/j.ijreses.2021.v18.a3609

measurement in the field employing regression analysis (Ostadhashemi et al., 2014; Stickler et al., 2009; Van Pham et al., 2019; Vargas-Larreta et al., 2017).

Remote sensing capabilities in estimating AGB and carbon stocks have been an area of interest in recent decades for several reasons, including their ability to extrapolate to vegetation parameters such as canopies, layer structures, leaves, and even forest floors; their wide area coverage, which increases their effectiveness and efficiency in AGB estimates and carbon stocks (Laurin et al., 2018); as well as the fact that remote sensing is also very helpful in mapping areas that have very limited access, with the support of spatial and temporal aspects (Lu, 2006).

Several methods of estimating AGB and carbon stocks using remote sensing have been developed based on passive and active sensors (Laurin et al., 2018). Passive sensor utilisation has some limitations, such as it can only be utilised during the day, and is limited by cloud cover, smoke and/or aerosols, atmospheric influence, and limitations in the extraction of vegetation structure information (Berninger et al., 2018).

This makes active sensors a potential alternative as they can solve the limitations that passive sensors have in estimating AGB and carbon stocks. One of the remote sensing technologies with active sensors that has been widely used for AGB estimation and carbon stocks is synthetic aperture radar (SAR), in this case Sentinel-1 imagery.

SAR is able to operate under a variety of weather conditions, can function during the day and night, has the ability for volumetric measurement (Berger et al., 2019; Santi et al., 2017).

Samarinda City is one of the major cities on Kalimantan Island, but the availability of stands vegetation in green open space in the city is still below the minimum area standard according to UU No. 26 of 2007 *tentang Penataan Ruang* (Law No. 26 of 2007 on Spatial Planning (Effendi, 2019). This makes inventories, monitoring, and evaluation related to such vegetation, along with derivative information produced from green open space, an important issue to deal with, including that of carbon stock.

The extensive cloud cover conditions in Samarinda City make optical imagery from passive system remote sensing recording relatively difficult to use in estimating carbon stocks, so active remote sensing, in this case Sentinel-1, which produces SAR imagery, can be used to solve the problem.

2 MATERIALS AND METHODOLOGY

2.1 Location and Data

The research site was located in Samarinda City, with coordinates 117°03'00" E – 117°18'14" E and 00°19'02" S – 00°42'34" S. The city was chosen as the research site because it has extensive cloud cover that occurs throughout the year, so SAR is expected to make an important contribution to this research. In addition, the geographical location of Samarinda City is relatively close to the prospective capital of the Republic of Indonesia located in Penajam Paser Utara Regency.

This has the potential to make physical development in Samarinda City more significant, which could affect the existence of stands vegetation in green open space.

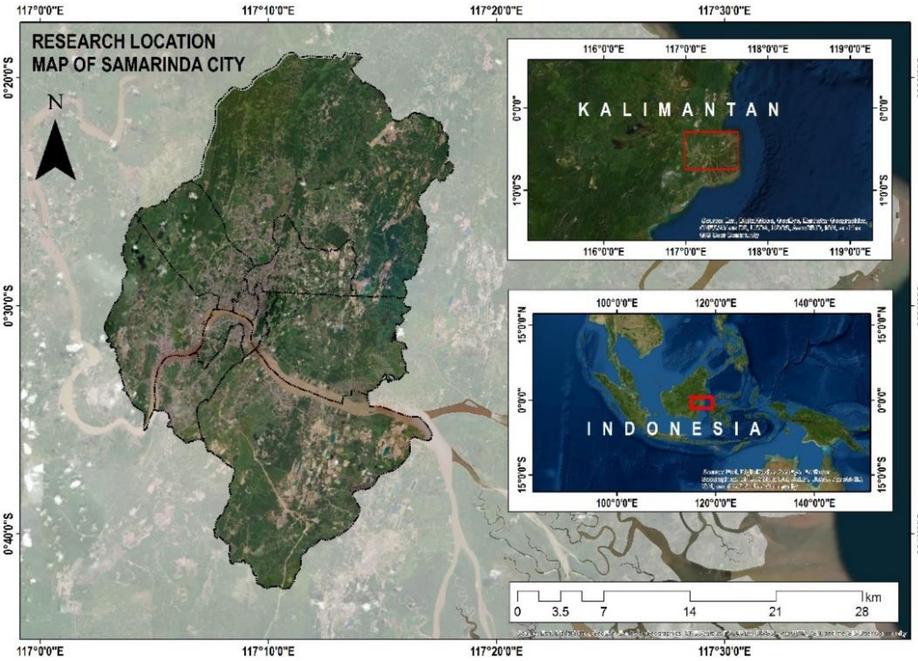

Figure 2-1: Map of Research Site

The data used to support the study included Sentinel-1A IW GRD image recording from January 15th 2021; Sentinel-2A L2A image recording from throughout 2020; an RBI digital map of Samarinda City, scale 1:50,000; and ALOS PALSAR Digital Elevation Model 12.5 m.

2.2 Data Preprocessing

Pre-processing of the Sentinel-1A SAR imagery included radiometric calibration; terrain correction using ALOS PALSAR DEM 12.5 m, including radiometric terrain flattening and radiometric terrain correction; and speckle filtering. Sentinel-1A IW GRD is a SAR imagery that has been projected against the Earth's ellipsoid model, but needs to be enforced/orthorectified in the terrain correction process because the geometry position is inverted horizontally (Amriyah et al., 2019).

Sentinel-2A L2A is an imagery that has been radiometrically corrected to surface reflectance or bottom-of-atmosphere reflectance and has been geometrically corrected. The pre-processing was performed by displaying road network vector data from the RBI map on the image for geometry position checking and histogram display to observe the distribution of reflectance image values, as well as by performing cloud masking throughout 2020 utilising Google Earth Engine (GEE). The utilisation of GEE in the cloud masking was intended to reduce compute loads and improve data processing efficiency due to the large number of image scenes.

2.3 Supervised Classification of Land Cover Extraction

Land cover extraction was performed to obtain the appearance of stands vegetation using the maximum likelihood algorithm. This was chosen based on its good performance in classifying land cover based on probability calculation or the maximum probability of each sample group (Danoedoro, 2012).

Five land cover classes were mapped in the study, namely stands vegetation, non-stands vegetation, built-up areas, bare land, and water bodies. The results of the land cover classification were masked to separate the stands vegetation class and other classes of land cover for further analysis.

2.4 Accuracy Assessment of Land Cover Classification

Land cover accuracy assessment was made by utilising a confusion matrix and kappa coefficient. The matrix was used to ascertain the level of reliability, or simply to establish the magnitude of errors or misclassification in the sample used (Sutanto, 2016). The kappa coefficient was used to assess the level of agreement from two points of view of the assessor in terms of classifying an object or data (Cohen, 1960), in this case the results of the land cover classification.

Determination of the accuracy of the assessment samples was made by utilising stratified random sampling techniques, in accordance with the land cover class. The sample used for the accuracy test was calculated by employing Slovin's formula in equation 2-1, following Sugiyono (2016), while the agreement level was measured using the kappa coefficient developed by Cohen (1960) in equation 2-2.

$$n = \frac{N}{1 + Ne^2} \qquad (2\text{-}1)$$

where:

n = number of samples

N = size of population

e = margin of error

$$k = \frac{N \sum_{i=1}^{n} m_{i,i} \; - \sum_{i=1}^{n}(G_i C_i)}{N^2 - \sum_{i=1}^{n}(G_1 C_i)} \qquad (2\text{-}2)$$

where:

k = Kappa coefficient

N = number of accuracy samples

$\sum_{i=1}^{n}(m_{i,i})$ = number of correct samples

$\sum_{i=1}^{n}(G_i C_i)$ = number of lines and columns multiplied per land cover class

2.5 Carbon Stock Estimation

Estimation of the carbon stocks was made on the stands vegetation using allometric equations to obtain biomass content, and conversion formulas to obtain carbon stocks. The study used the allometric equation developed by Brown (1997), especially for use in humid-climate tropical vegetation. It was chosen because climatic conditions in Samarinda City include varied rainfall, from 31.8 - 401.7 mm/month and with humidity reaching 85% (Central Bureau of Statistics, 2019).

Another factor underlying the selection of the equation was the number of samples, which totalled 170 with varied tropical vegetation species. They were more in accordance with the ability of Sentinel-1A SAR imagery related to its spatial resolution which spatially finds it quite difficult to accommodate the appearance of vegetation up to the level of species.

The estimation of stands vegetation carbon stocks was derived from 47% of the total content of aboveground biomass (Asner and Mascaro, 2014; IPCC, 2006 in Zaki et al., 2016). The equation used for the estimation of carbon stocks is presented as equation 2-3 :

$$AGC = AGB \times 0{,}47 \qquad (2\text{-}3)$$

where:

AGC = aboveground carbon stock (tons/pixel)

AGB = aboveground biomass (tons/pixel)

2.6 Statistical Analysis

The study used parametric inferential statistical analysis in the form of Pearson product-moment correlation analysis, simple linear regression analysis, simple non-linear regression analysis consisting of polynomial and exponential models, r-Pearson correlation tests, partial T-tests, and ANOVA tests.

The response variable (Y) used in the study was the field carbon stock, while the predictor variable (X) was the SAR backscatter value. Pearson product-moment correlation analysis using the Pearson equation refers to Walpole (1995), as presented in equation 2-4 **:**

$$Cor = \frac{n\,\Sigma XY - (\Sigma X)(\Sigma Y)}{\sqrt{\{n\Sigma X^2 - (\Sigma X^2)\}} - \sqrt{\{n\Sigma Y^2 - (\Sigma Y^2)\}}} \quad (2\text{-}4)$$

where:

Cor = Pearson correlation coefficient (r)
n = number of samples
X = backscatter value (dB)
Y = carbon stock value (tons/pixel)

The regression analysis was performed using simple linear regression and simple non-linear regression, with polynomial and exponential models.

2.7 Sampling Techniques and Sample Plot Size

The determination of samples in the field was made using the stratified random sampling technique, based on the distribution of backscatter values divided into five classes, but the implementation in the field encountered various obstacles.

These included difficult access to the sample location, especially in the north and south of Samarinda City, due to the terrain in the form of hilly to mountainous forests. In addition, the distance between the samples was quite far, thus reducing the efficiency of the field work, and limiting the facilities and infrastructure supporting the field. There were also limitations related to human resources, climatic factors, especially high rainfall that hindered the sampling process, and the policy of the Enforcement of Restrictions on Community Activities in the administrative area of East Kalimantan Province, especially in Samarinda City.

Based on these constraints, the sampling technique was changed to purposive sampling, with the aim of accommodating the obstacles faced, and prioritising safety and security factors, both physical and social. Attention was also paid to the effectiveness and efficiency of the field work and to the spatial distribution of the samples taken. This allowed the collection of samples in the field to meet the planned targets.

The sample plot size was created with reference to McCoy (2005, in Pratama, 2019), assuming the potential for geometric position shifting of the image represented by a root mean square error (RMSE) value of 0.5 pixels from the starting position. This was done in anticipation of geometric position shifts; the measured field samples were still included in the image pixel size. The equation used for the sample plot size is presented as equation 2-5 :

$$A = P\,(1 + 2L) \quad (2\text{-}5)$$

where:

A = sample plot size in the field (m^2)
P = spatial resolution (m)
L = root mean square error (RMSE)

2.8 Accuracy Assessment of the Carbon Stock Estimation Model

The method used to test the accuracy of the model was standard error of estimate (SEE). This determined the number of estimated errors generated on each sample by comparing the estimated results and field data in the accuracy test sample. The formula used is shown as equation 2-6 (Margaretha, 2013, in Pratama, 2019).

$$SE = \sqrt{\frac{\Sigma(y - y')^2}{n - 2}} \quad (2\text{-}6)$$

where:

SE = standard error of estimate (tons/pixel)
$\Sigma(y-y')^2$ = total difference between values of carbon stock in the accuracy sample and field values
n = number of accuracy samples

3 RESULTS AND DISCUSSION

3.1 Land Cover Classification

The classification of land cover was made using Sentinel-2A imagery that was filtered using a cloud masking algorithm. This is because Samarinda City has extensive cloud cover throughout the year, so cloud masking algorithms are needed to clean up, or at least suppress the dominance of cloud appearance on images. Based on Figure 3-1, the distribution of the visually built-up area is seen to be clustered in the central part of Samarinda City. Bare land is quite spread out in the southern part of the city, with a small part to the east. The bare land is quite extensive and dominated by land from disused coal mines and ones that are still actively operating. The stands vegetation is quite extensively distributed in the north, east, and southern parts of Samarinda City.

The area is dominated by wild forests/wild habitats and some points are sites of revegetation of former coal mine land. The most visible water body is the Mahakam River, and to a lesser extent dams, lakes, and water basins of former coal mines. The stands vegetation on green open space is separated from other land cover classes as material for masking Sentinel-1A imagery.

3.2 Accuracy Assessment of Land Cover Classification

The results of the land cover accuracy test showed an accuracy value of 88.83%, with a kappa coefficient of 0.8427. According to Anderson (1971, in Anderson et al., 1976), the minimum acceptable accuracy of remote sensing data classification results is 85%. Based on that, the accuracy in this case of 88.83% is acceptable for use in the subsequent analysis.

The agreement rate of accuracy measured from the kappa coefficient also showed a very strong level, with a kappa coefficient value of 0.8427. This shows that the accuracy value obtained was not on the basis of chance (accidental). Based on the accuracy and coefficient of kappa obtained, extracted land cover could be used for further analysis in the study. The accuracy test results are presented in Table 3-1.

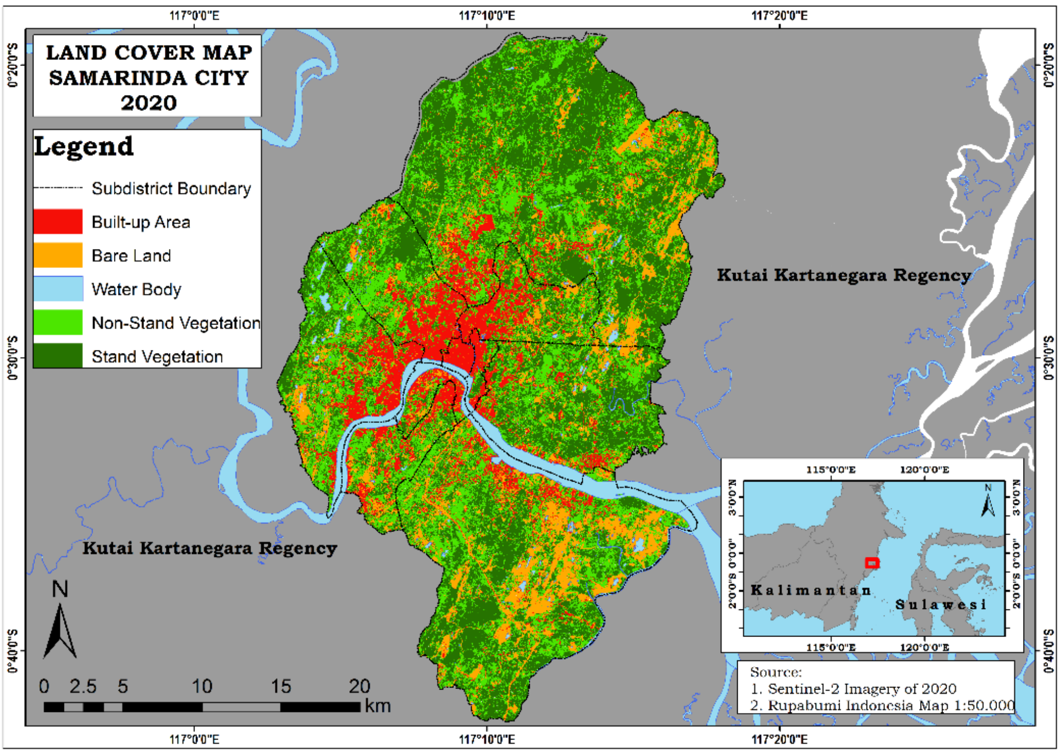

Figure 3-1: Land Cover Map of Samarinda City

Table 3-1: Confusion Matrix of Land Cover Classification

		Reference						
		Built-up Area	Bare Land	Water Body	Non-stands Vegetation	Stands Vegetation	Total line	User Acc. (%)
Tentative	Built-up Area	39	3	0	1	0	43	90.70
	Bare Land	9	48	1	0	0	58	82.76
	Water Body	0	0	14	0	0	14	100.00
	Non-stands Vegetation	0	0	0	105	14	119	88.24
	Stands Vegetation	0	0	0	16	144	160	90.00
	Total Column	48	51	15	122	158	394	
	Producer Acc. (%)	81.25	94.12	93.33	86.07	91.14		
	Omission Error (%)	18.75	5.88	6.67	13.93	8.86		
	Total Acc. (%)	88.83						
	Kappa Coefficient	0.843						

3.3 Statistical Analysis

3.3.1 Data Normalization

It is important to perform data normality tests as a consequence of the use of parametric inferential analysis techniques that require normal distributed data assumptions. In this case, normality tests were conducted qualitatively using histograms, normal curves and probability plots, and quantitative normality tests were performed using Kolmogorov-Smirnov. Based on Figure 3-2 (a), it can be seen that the sample dataset is mostly within the normal curve. This shows that the sample dataset is distributed normally. Some data appear to be out of the range of normal curves, which indicates outlier data or an overestimated value compared to the overall sample dataset. Based on Figure 3-2 (b), it can be seen that the data distribution is grouped on a 1:1 plot line. This shows that the sample dataset used is distributed normally, based on the interpretation of the 1:1 line on the probability plot.

The assessment of data normality using Kolmogorov-Smirnov was conducted by comparing the distribution of data in the sample and the raw distribution, and comparing the distribution of data in the sample and the error margin (α) of 0.05. Distributed data are normal when the distribution of the data in the sample (diff, max) < the raw distribution (diff, α), and/or the distribution of data in the sample (diff, max) > α. The results of the normality test data using Kolmogorov-Smirnov are presented in Table 3-2.

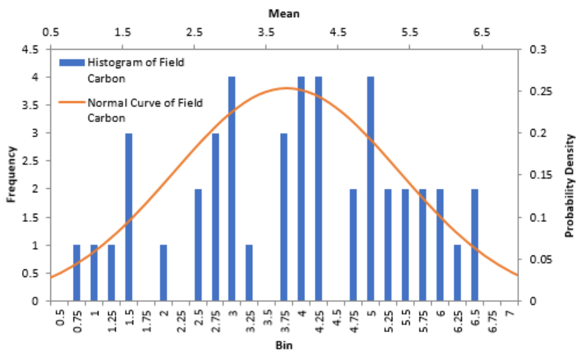

(a)

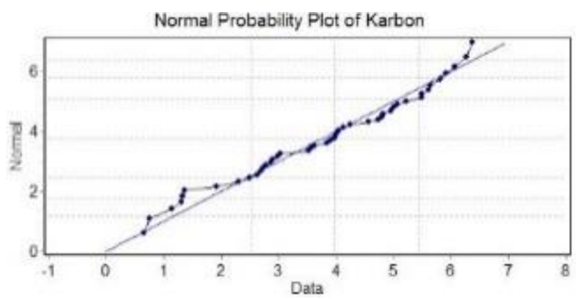

(b)

Figure 3-2: (a) Histogram and normal curve, (b) Probability plot

Table 3-2: Normality test results using Kolmogorov-Smirnov

Sample Dataset	Number of Samples	Diff, max	Diff,α	α	Description
VH	45	0.0529	0.200	0.05	Normal distribution
VV		0.0617			Normal distribution
Field Carbon Stock		0.0683			Normal distribution

Based on Table 3-2, it can be seen that the data distribution values in all the sample datasets have a maximum value (diff, max) < the standard distribution (diff, α) of 0.200, in addition to the distribution of data in the sample (diff, max) > an error margin (α) of 0.05. This ensures that the sample dataset used has been distributed normally.

3.3.2 Correlation and Regression Analysis

Correlation analysis was conducted using Pearson's product-moment correlation on the predictor variables (X) and response variables (Y) on all three regression models, namely the simple linear, exponential, and polynomial. Table 3-3 presents the correlation and determination coefficients of all three regression modelsBased on Table 3-3, it can be seen that the three regression models with VH and VV polarisation had a positive correlation coefficient (r) with carbon stocks. The correlation strength in VH polarisation was in the strong category, apart from the exponential regression models, while in VV polarisation, all three regression models had correlation forces within the moderate category. VH polarisation also had a higher coefficient of determination (r^2) than that of VV. The highest coefficient of determination was obtained by the polynomial regression model at VH polarisation of 0.4717. This suggests that the value of the backscatter in the polynomial regression model can model a carbon stock of 47.17%, while 52.83% was influenced by factors other than this value.

Significance tests were conducted using a T-partial test and an F-simultaneous, or ANOVA, test. The partial T-test was performed by comparing the t-count value with the t-table value, while the F-simultaneous, or ANOVA, test was performed by comparing the F-significance value with the α value. Table 3-4 presents the results of the significance test.

Table 3-3: Correlation and determination coefficients of all three regression models

Polarization	Regression Model	Correlation Coefficient (r)	Determination Coefficient (r^2)	Category
VH	Simple Linear	0.686	0.471	Strong correlation
	Exponential	0.673	0.452	Moderate correlation
	Polynomial	0.687	0.472	Strong correlation
VV	Simple Linear	0.579	0.299	Moderate correlation
	Exponential	0.574	0.330	Moderate correlation
	Polynomial	0.547	0.335	Moderate correlation

Table 3-4: Significance test results

Polarisation	Number of Samples	T-count	T-table	F-significance	α
VH	45	6.113	2.015	2.73E-07	0.05
VV		4.230		0.000124	

From Table 3-4, it can be seen that the t-count value > the t-table value on both polarisations, which indicates that the backscatter value for both polarisations significantly affects the value of carbon stocks. The significance test was also reinforced by the F-simultaneous, or ANOVA, test, in which the F-significance value < the α value, indicating that the predictor variable, in which in this case the backscatter value, had a significant influence on the response variable in the form of carbon stock.

3.4 Carbon Stock Estimation Model and Accuracy Assessment

The carbon stock estimation model was built on a sample of models that have been tested for normality and data significance, so it was expected to represent the original condition as best as possible. Modelling of carbon stock estimates was made by applying the regression equations that were obtained from the Sentinel-1A images. The regression equations used are presented in Table 3-5.

The application of the regression equations shown in Table 3-5 produced an estimated model of carbon stocks with different total estimates. The total estimate of these indicates different sensitivities in the backscatter value to carbon stocks, especially with different polarisations. The regression model used to model the carbon stocks was conceptually adapted to the characteristics of the backscatter values in the samples used. The total estimated carbon stock of the three regression models with VH polarisation has a lower estimated value than that of VV.

Based on the data, it is evident that the exponential models in both polarisations consistently obtained the lowest total estimated carbon stock compared to the other two regression models. The accuracy test results are presented in Table 3-6

Based on Table 3-6, it can be seen that the accuracy of the model varies considerably, with the highest accuracy value obtained by exponential models with VH polarisation of 87.6% and estimated errors of 0.57 tons/pixel. The lowest model accuracy was obtained by polynomial models with VV polarisation, an accuracy value of 13.1%, and an estimated error of 4.01 tons/pixel.

Table 3-5: Regression equation for carbon stock estimation model

Polarization	Regression Model	Regression Equation	Carbon Stock (Tons)
VH	Simple Linear	$Y = 0.6568x + 10.519$	7,248,978.9
	Exponential	$Y = 34.579e^{0.2279x}$	6,489,478.1
	Polynomial	$Y = 0.0157x^2 + 0.9768x + 12.106$	6,974,219.9
VV	Simple Linear	$Y = 0.55333x + 6.2232$	7,625,805.9
	Exponential	$Y = 8.2751e^{0.1789x}$	7,100,536.5
	Polynomial	$Y = -0.0923x^2 - 0.2449x + 4.7211$	7,666,575.7

Table 3-6: Model accuracy test results

Polarisation	Regression Model	Estimated Error (tons/pixel)	Maximum Accuracy (%)	Minimum Accuracy (%)
VH	Simple Linear	1.27	72.4	59.9
	Exponential	0.57	87.6	82.1
	Polynomial	0.89	80.7	71.9
VV	Simple Linear	1.30	71.8	58.9
	Exponential	1.01	78.2	68.2
	Polynomial	4.01	26.5	13.1

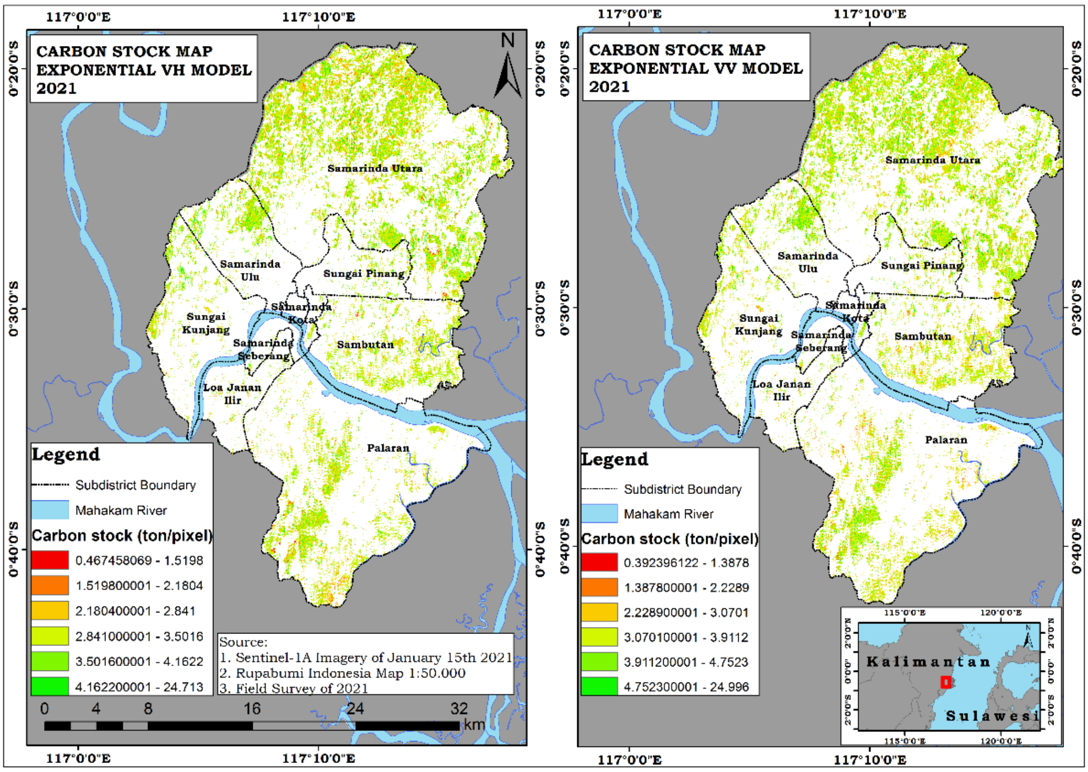

(a) (b)

Figure 3-3: (a) VH exponential model carbon stock map and (b) VV exponential model carbon stock map

The exponential VV and VH polarisation models were recorded to have the highest accuracy compared to the others. This showed consistency in the exponential models in modelling carbon stocks; previously, the total estimated value of exponential model carbon stocks in both polarisations also had the lowest value compared to the other two models.

Visually, the spatial distribution ofstands vegetation tends to be grouped in the northern and southern parts of Samarinda City. Higher carbon stock classes tend to be distributed in the northern part of the city, which is administratively located in North Samarinda Subdistrict and part of Samarinda Ulu Subdistrict. This is because the area has vegetation with typology ranging from wild forests/ habitats to urban forests, so the distribution is quite extensive compared to other subdistricts. The spatial distribution of carbon stocks can be seen in Figure 3.

4 CONCLUSION

The results show that the estimated carbon stock on the surface using the VH exponential model was 6,489,478.1 tons, with an accuracy of 87.6% and an estimated error of 0.57 tons/pixels, while the exponential VV models produced a figure of 7,100,536.5 tons with an accuracy of 78.2% and an estimated error of 1.01 tons/pixel. Distributed carbon stocks tend to group to the north, south, and east, and to a lesser extent to the west of the city. Administratively, spatial distribution of carbon stock is extensively distributed in North Samarinda, Samarinda Ulu, Sambutan, and Palaran subdistricts.

ACKNOWLEDGEMENTS

The authors thank the European Space Agency, ASF Alaska, and the Geospatial Information Agency for the research data support.

AUTHOR CONTRIBUTIONS

Estimation of aboveground carbon stock using SAR Sentinel-1 imagery in

Samarinda City. Lead Author: Bayu Elwantyo Bagus Dewantoro, Co-Author: Retnadi Heru Jatmiko.

REFERENCES

Amriyah, Q., Rahmat. A., Haris, S. D., & Rachmat, M. (2019). Analisis Perbandingan Data Level-1 Sentinel 1A/B (Data SLC dan GRD) menggunakan *Software* SNAP dan GAMMA [Comparative Analysis of Level-1 Sentinel 1A/B Data (Data SLC and GRD) using SNAP and GAMMA Software]. Seminar Nasional Penginderaan Jauh ke-6 Lembaga Penerbangan dan Antariksa Nasional (LAPAN).

Anderson, J. R. (1971). Land Use Classification Schemes Used in Selected Recent Geographic Applications of Remote Sensing. *Photogrammetric Engineering, 37*(4), 379 - 387.

Anderson, J. R., Hardy, E. E., Roach, J. T., & Witmer, R. E. (1976). A Land Use and Land Cover Classification System for Use with Remote Sensor Data. *Geological Survey Professional Paper 964.*

Asner, G. P & Mascaro, J. (2014). Mapping Tropical Forest Carbon: Calibrating Plot Estimate To A Simple Lidar Metric. *Remote Sensing of Environment* (140), 614 – 624.

Badan Pusat Statistik Kota Samarinda [Central Bureau of Statistics]. (2019). Kecamatan Sungai Pinang Dalam Angka Tahun 2019 [Sungai Pinang Subdistrict in Figure Year 2019]. Samarinda: BPS Kota Samarinda.

Berger, C., Werner, S., Wigley-coetsee, C., Smit, I., & Schmullius, C. (2019). Multi-Temporal Sentinel-1 Data for Wall-To-Wall Herbaceous Biomass Mapping In Kruger National Park , South Africa — First Results. *IEEE Geoscience and Remote Sensing Symposium 2019*, 7358–7360.

Berninger, A., Lohberger, S., Stängel, M., & Siegert, F. (2018). SAR-Based Estimation of Above-Ground Biomass and Its Changes in Tropical Forests of Kalimantan Using L- and C-Band. *Remote Sensing, 10*(6). https://doi.org/10.3390/rs10060831.

Brown, S. (1997). *Estimating Biomass and Biomass Change of Tropical Forests: a Primer.* Roma: FAO.

Chave, J., Rejou-Mechain, M., Burquez, A., Chidurnayo, E., Colgan, M. S., Delliti, ... Vielledent, G. (2014). Improved Allometric Models to Estimate The Aboveground Biomass of Tropical Trees. *Global Change Biology, 20*(10), 3177 – 3190. https://doi.org/10.1111/gcb.12629.

Cohen, J. (1960). A Coefficient of Agreement for Nominal Scales. *Educational and Psychological Measurement,* 60, 27 - 46.

Danoedoro, P. 2012. *Pengantar Penginderaan Jauh Digital* [Introduction to Digital Remote Sensing]. Yogyakarta: Andi.

Effendi, J. (2019). Implementasi Peraturan Daerah Nomor 2 Tahun 2014 tentang Rencana Tata Ruang Wilayah Terkait Pelaksanaan Ruang Terbuka Hijau di Kota Samarinda [Implementation of Regional Law No. 2 of 2014 on Regional Spatial Planning in Green Open Space Realization in Samarinda City]. Thesis [Master's Thesis]. Yogyakarta: Fakultas Hukum [Faculty of Law], Universitas Islam Indonesia.

Fonseca, W., Alice, F. E., & Rey-Benayas, J. M. (2012). Carbon Accumulation in Aboveground and Belowground Biomass and Soil of Different Age Native Forest Plantations In The Humid Tropical Lowlands of Costa Rica. *New Forests, 43*(2), 197–211. https://doi.org/10.1007/s11056-011-9273-9.

Godwin, C., Chen, G., & Singh, K. K. (2015). The Impact Of Urban Residential Development Patterns On Forest Carbon Density: An Integration of LiDAR, Aerial Photography and Field Mensuration. *Landscape and Urban Planning*, *136*, 97–109. https://doi.org/10.1016/j.landurbplan.2014.12.007

IPCC. (2006). IPCC Guidelines for National Greenhouse Gas Inventories. Hayama, Kanagawa: *Institute for Global Environmental Strategies* (IGES).

Jo, H. K. (2002). Impacts of Urban Greenspace On Offsetting Carbon Emissions For Middle Korea. *Journal of Environmental Management*, *64*(2), 115–126. https://doi.org/10.1006/jema.2001.0491

Krooks, A., Kaasalainen, S., Kankare, V., Joensuu, M., Raumonen, P., & Kaasalainen, M. (2014). Tree Structure Vs. Height From Terrestrial Laser Scanning And Quantitative Structure Models. *Silva Fennica*, *48*(2), 1–11. https://doi.org/10.14214/sf.1125

Laurin, G. V., Balling, J., Corona, P., Mattioli, W., Papale, D., Puletti, N., Rizzo, M., Truckenbrodt, J., & Urban, M. (2018). Above-ground Biomass Prediction By Sentinel-1 Multitemporal Data In Central Italy With Integration Of ALOS-2 And Sentinel-2 Data. *Journal of Applied Remote Sensing*, *12*(01), 1 - 18. https://doi.org/10.1117/1.jrs.12.016008

Lu, D. (2006). The Potential And Challenge Of Remote Sensing-Based Biomass Estimation. *International Journal of Remote Sensing*, *27*(7), 1297–1328. https://doi.org/10.1080/01431160500486732.

Margaretha, E. W. (2013). Estimasi Cadangan Karbon Vegetasi Tegakan di Kota Yogyakarta dan Sekitarnya Berbasis ALOS AVNIR-2 [Aboveground Carbon Stock Estimation of Stand Vegetation in Yogyakarta using ALOS AVNIR-2]. Skripsi [Bachelor Thesis]. Yogyakarta: Fakultas Geografi [Faculty of Geography]. Universitas Gadjah Mada.

McCoy, R. M. (2005). *Field Methods in Remote Sensing*. New York: The Guilford Press. http://doi.wiley.com/10.1111/j.1541-0064.2006.00161_2.x.

Ostadhashemi, R., Shahraji, T. R., Roehle, H., & Limaei, S. M. (2014). Estimation of Biomass And Carbon Storage Of Tree Plantations In Northern Iran. *Journal of Forest Science*, *60*(9), 363–371. https://doi.org/10.17221/55/2014-jfs.

Pratama, L. D. Y. 2019. Model Estimasi Stok Karbon Atas Permukaan Tegakan Karet (*Hevea brasiliensis*) menggunakan Citra Sentinel 2A Kasus di Perkebunan Karet PTPN IX Kebun Ngobo dan Kebun Getas, Kabupaten Semarang [Aboveground Carbon Stock Estimation Model of Rubber Plantations (*Hevea brasiliensis*) using Sentinel 2A Imagery, Case: PTPN IX Ngobo and Getas Plantations Area, Semarang Regency]. Skripsi [Bachelor's Thesis]. Yogyakarta: Fakultas Geografi [Faculty of Geography]. Universitas Gadjah Mada.

Poudyal, N. C., Siry, J., & Bowker, J. M. (2011). Urban Forests And Carbon Markets: Buyers' Perspectives. *Journal of Forestry*, *109*(7), 378–385. https://doi.org/10.1093/jof/109.7.378

Santi, E., Paloscia, S., Pettinato, S., Fontanelli, G., Mura, M., Zolli, C... Chirici, G. (2017). The Potential Of Multifrequency SAR Images For Estimating Forest Biomass In Mediterranean Areas. *Remote Sensing of Environment*, *200*(February), 63–73. https://doi.org/10.1016/j.rse.2017.07.038

Sidiq, W. (2013). Pemanfaatan Penginderaan Jauh dan Sistem Informasi Geografis untuk Evaluasi dan Arahan Pengembangan Ruang Terbuka Hijau di Kota Semarang [Utilization of Remote Sensing and Geographic Information System for Evaluation and Recommendation of Green Open Space Development in Semarang City]. Skripsi [Bachelor's Thesis]. Yogyakarta: Fakultas Geografi [Faculty of Geography]. Universitas Gadjah Mada.

Stickler, C. M., Nepstad, D. C., Coe, M. T., McGrath, D. G., Rodrigues, H. O., Walker, W. S., Soares-Filho, B. S., & Davidson, E. A. (2009). The Potential Ecological Costs And Cobenefits Of REDD: A Critical Review And Case Study From The Amazon Region. *Global Change Biology*, *15*(12), 2803–2824. https://doi.org/10.1111/j.1365-2486.2009.02109.x

Strohbach, M. W., & Haase, D. (2012). Above-ground Carbon Storage By Urban Trees In Leipzig, Germany: Analysis Of Patterns In A European City. *Landscape and Urban Planning*, *104*(1), 95–104. https://doi.org/10.1016/j.landurbplan.2011.10.001

Sugiyono. (2016). Metode Penelitian Kuantitatif, Kualitatif, dan R&D [Quantitative, Qualitative, and R&D Research Method]. Bandung: Alfabeta.

Sutanto (2016). *Metode Penelitian Penginderaan Jauh* [Research Method of Remote Sensing]. Edisi Revisi [Revision Ed.]. Yogyakarta: Ombak.

Tavasoli, N., Arefi, H., Samiei-Esfahany, S., & Ronoud, Q. (2019). Modelling the Amount Of Carbon Stock Using Remote Sensing In Urban Forest And Its Relationship With Land Use Change. *International Archives of the Photogrammetry, Remote Sensing and Spatial Information Sciences - ISPRS Archives*, *42*(4/W18), 1051–1058. https://doi.org/10.5194/isprs-archives-XLII-4-W18-1051-2019

Tobler, W. (1987). Measuring Spatial Resolution. *Proceedings: Land Resources Information Systems Conference, Beijing,* pp 12 – 16.

Van Pham, M., Pham, T. M., Viet Du, Q. V., Bui, Q. T., Van Tran, A., Pham, H. M., & Nguyen, T. N. (2019). Integrating Sentinel-1A SAR Data And GIS To Estimate Aboveground Biomass And Carbon Accumulation For Tropical Forest Types In Thuan Chau District, Vietnam. *Remote Sensing Applications: Society and Environment*, *14*(September 2017), 148–157. https://doi.org/10.1016/j.rsase.2019.03.003

Vargas-Larreta, B., López-Sánchez, C. A., Corral-Rivas, J. J., López-Martínez, J. O., Aguirre-Calderón, C. G., & Álvarez-González, J. G. (2017). Allometric Equations For Estimating Biomass And Carbon Stocks In The Temperate Forests Of North- Western Mexico. *Forests*, *8*(8), 1–20. https://doi.org/10.3390/f8080269

Walpole, R. E. (1995). *Pengantar Statistika Edisi ke-3* [Introduction to Statistics 3rd Ed.]. Jakarta: Gramedia.

Wang, V., & Gao, J. (2020). Estimation of Carbon Stock In Urban Parks: Biophysical Parameters, Thresholds, Reliability, And Sampling Load By Plant Type. *Urban Forestry and Urban Greening*, *55*, 126852. https://doi.org/10.1016/j.ufug.2020.126852

Zaki, N. A. M., Zulkiflee, A. L., & Mohd, Z. Z. (2015). Aboveground Biomass and Carbon Stock Estimation using Double Sampling Approach and Remotely Sensed Data. *Jurnal Teknologi* (*Sciences & Engineering*) Universiti Teknologi Malaysia, 78 (5-4), 57 – 62.